



This is a repository copy of *Development of a combined leaching and ion-exchange system for valorisation of spent potlining waste*.

White Rose Research Online URL for this paper:
<https://eprints.whiterose.ac.uk/157796/>

Version: Supplemental Material

Article:

Robshaw, T.J. orcid.org/0000-0002-9816-8236, Bonser, K., Coxhill, G. et al. (2 more authors) (2020) Development of a combined leaching and ion-exchange system for valorisation of spent potlining waste. *Waste and Biomass Valorization*, 11 (10). pp. 5467-5481. ISSN 1877-2641

<https://doi.org/10.1007/s12649-020-00954-1>

Reuse

Items deposited in White Rose Research Online are protected by copyright, with all rights reserved unless indicated otherwise. They may be downloaded and/or printed for private study, or other acts as permitted by national copyright laws. The publisher or other rights holders may allow further reproduction and re-use of the full text version. This is indicated by the licence information on the White Rose Research Online record for the item.

Takedown

If you consider content in White Rose Research Online to be in breach of UK law, please notify us by emailing eprints@whiterose.ac.uk including the URL of the record and the reason for the withdrawal request.



eprints@whiterose.ac.uk
<https://eprints.whiterose.ac.uk/>

Development of a combined leaching and ion-exchange system for valorisation of spent potlining waste

SUPPORTING INFORMATION

Thomas J. Robshaw, Keith Bonser, Glyn Coxhill, Robert Dawson and Mark D. Ogden

Information on Lanthanum-loaded Puromet™ MTS9501 resin (La-MTS9501)

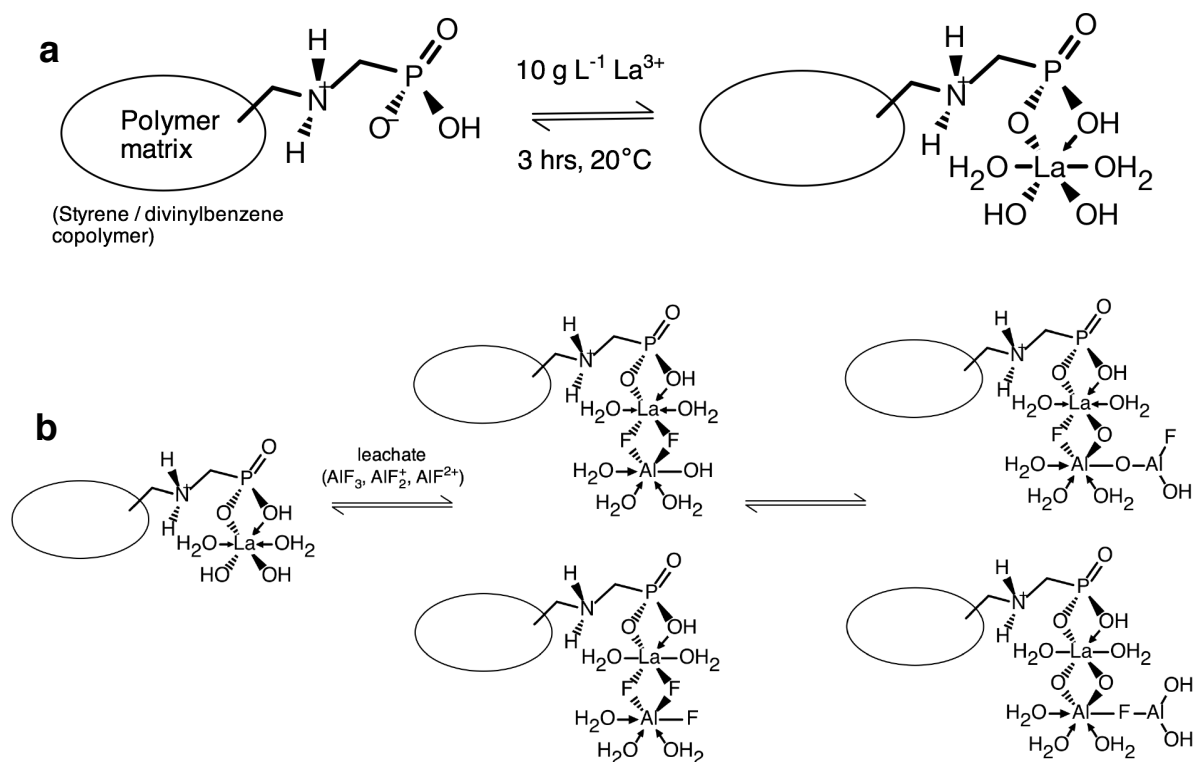


Figure S1. (a) La-loading mechanism for commercial resin Puromet™ MTS9501 resin, showing chelation of La ion to aminophosphonic acid functionality. (b) Probable mechanisms of aluminium hydroxyfluoride (AHF) uptake by La-MTS9501. Initial strong chemisorption interaction between La centre and aqueous AHF, then complexation with further weakly-bound AHFs (coordinating water ligands are omitted for clarity), accompanied by ligand-exchange reactions, resulting in the dominant bound AHF species having stoichiometry of $\sim\text{Al}(\text{OH})_2\text{F}$ [1, 2].

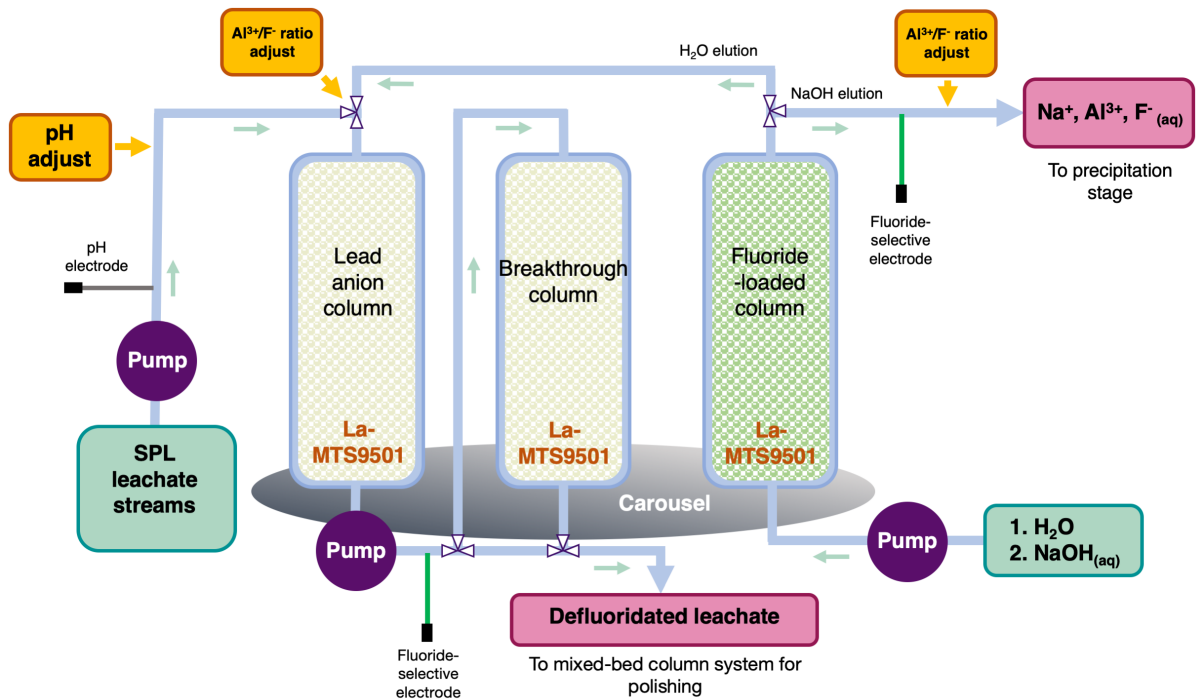


Figure S2. Conceptual diagram of La-MTS9501 column system for treatment of SPL leachate.

Images of selected SPL samples



Figure S3. Photographs of the three different unprocessed SPL samples selected for leaching trials. Sample A (left), containing a large fraction of cementitious and brick material. Sample B (middle), containing visible cementitious material. Sample C (right), appearing to be mainly graphitic material.

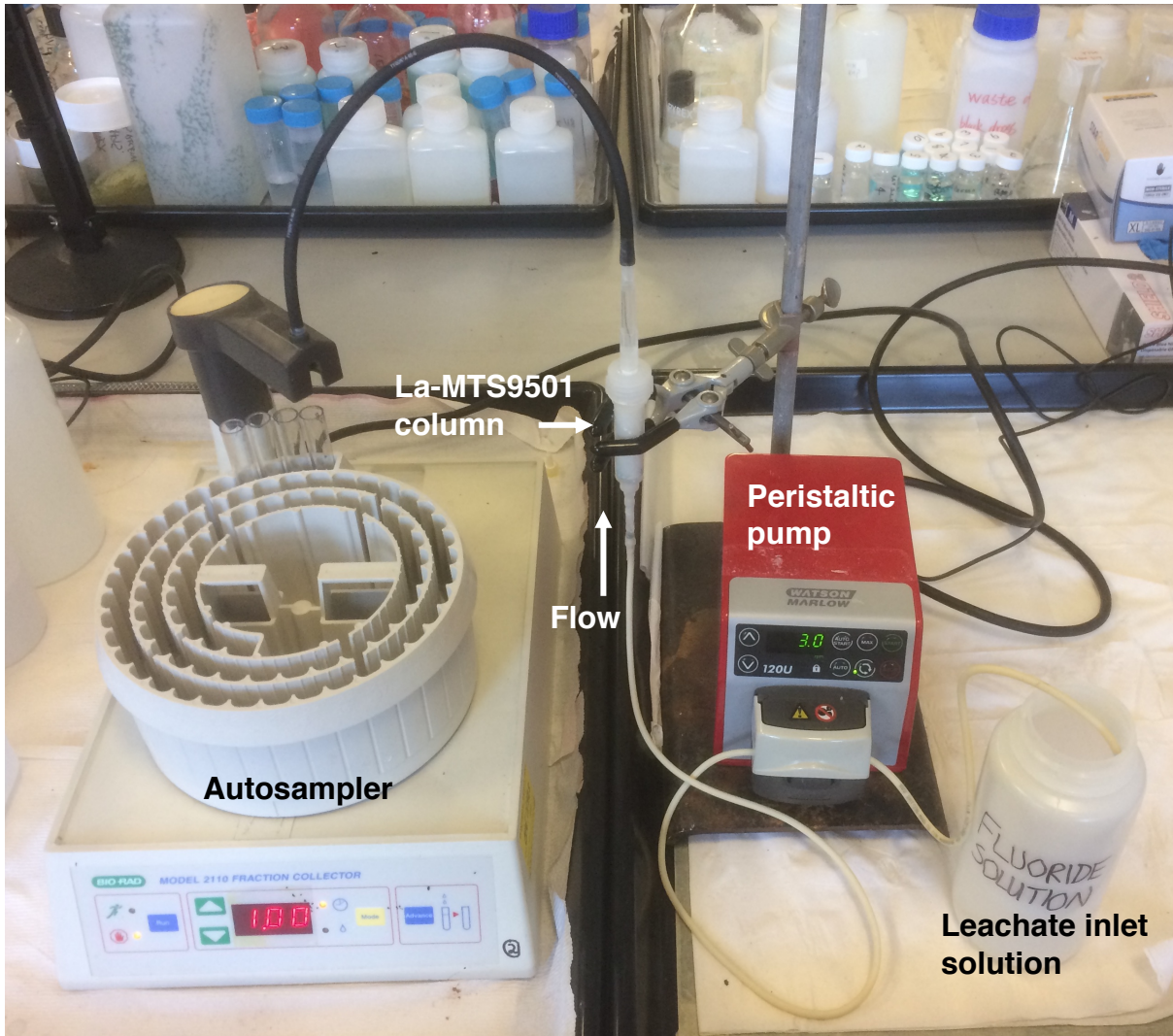


Figure S4. Experimental setup for a fixed-bed column fluoride-loading experiment.

Dynamic breakthrough models

Dose-response model [3]

$$\frac{C}{C_i} = 1 - \frac{1}{1 + \left(\frac{V_{ef}}{b}\right)^a} \quad (S1)$$

$$q_0 = \frac{bC_i}{m} \quad (S2)$$

In these equations C is the fluoride concentration in the effluent at a given time (mg L^{-1}), C_i is the fluoride concentration in the effluent at full breakthrough (mg L^{-1}), V_{ef} is the volume of solution eluted from the column (mL), a and b are constants of the Dose-Response model, q_0 is the theoretical maximum uptake capacity of the resin in a dynamic environment (mg g^{-1}) and m is the dry mass of resin (g).

Thomas model [4]

$$\frac{c}{c_i} = \frac{1}{1 + e^{\left(\frac{k_{Th}}{Q}\right)(q_0 m - c_i V_{ef})}} \quad (S3)$$

where k_{Th} = Thomas rate constant ($\text{mL min}^{-1} \text{mg}^{-1}$), Q = flow rate (mL min^{-1}). All other terms as previously described.

Yoon-Nelson model [5]

$$\frac{c}{c_i} = \frac{1}{1 + e^{k_{YN}(\tau - t)}} \quad (S4)$$

where k_{YN} = Yoon-Nelson rate constant (min^{-1}), t = time (min) and τ = the time at which $C/C_i = 0.5$ (min). All other terms as previously described. It should be noted that the Thomas and Yoon-Nelson models are mathematically analogous. Therefore, their fitting to experimental data using Microsoft SOLVER [6] produces identical R^2 values.

PXRD spectra of SPL samples at various process stages

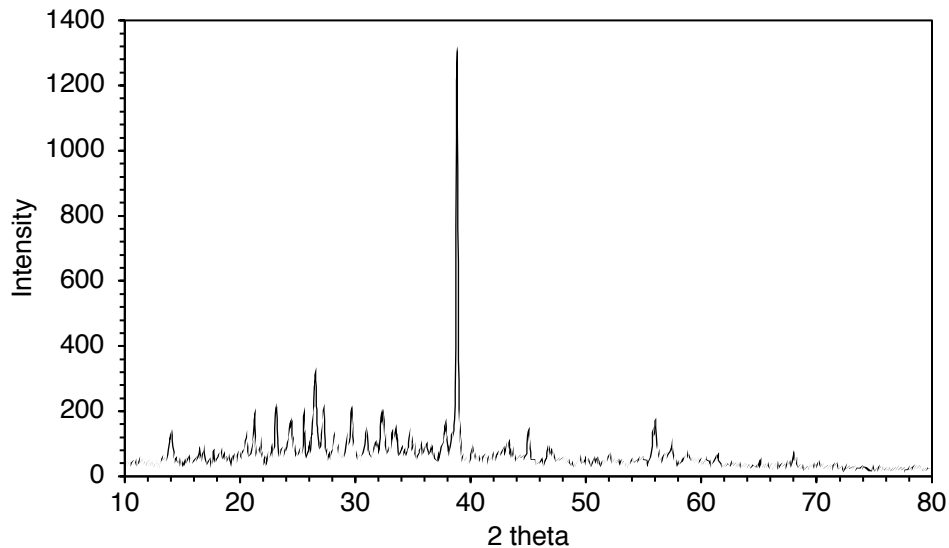


Figure S5. PXRD spectrum of sample A <1.18 mm size fraction as received.

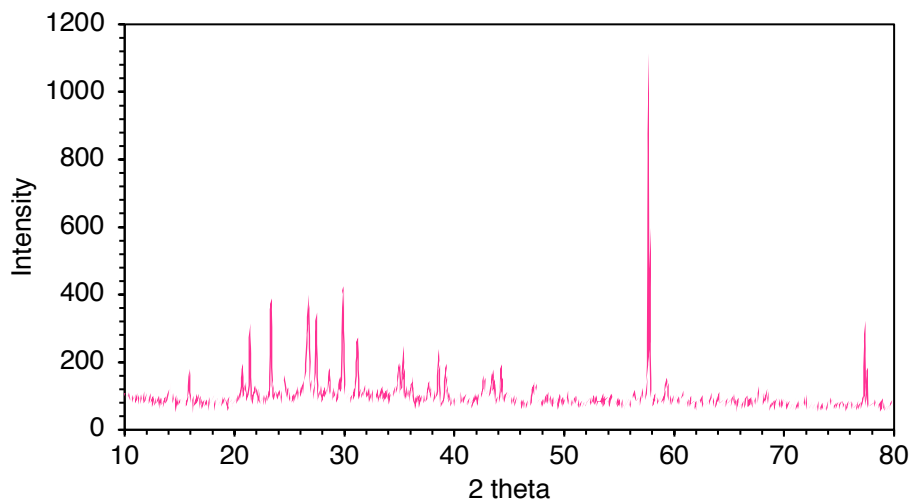


Figure S6. PXRD spectrum of sample A <1.18 mm size fraction after caustic leaching treatment.

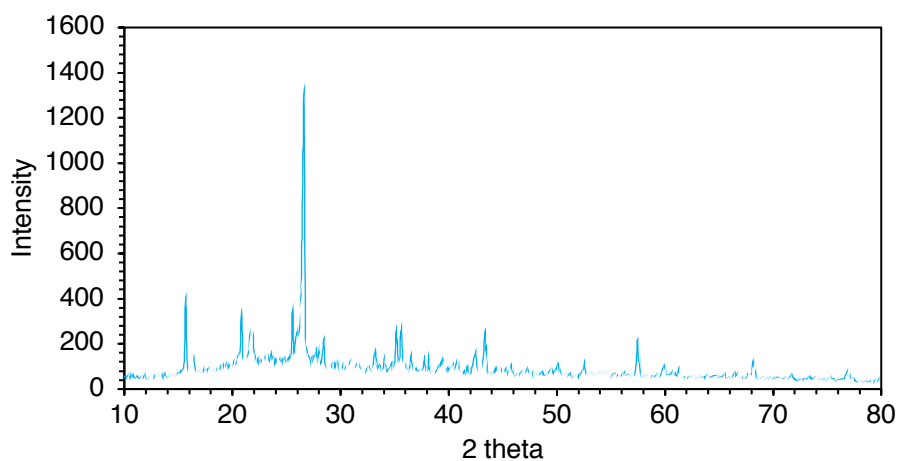


Figure S7. PXRD spectrum of sample A <1.18 mm size fraction after full leaching treatment.

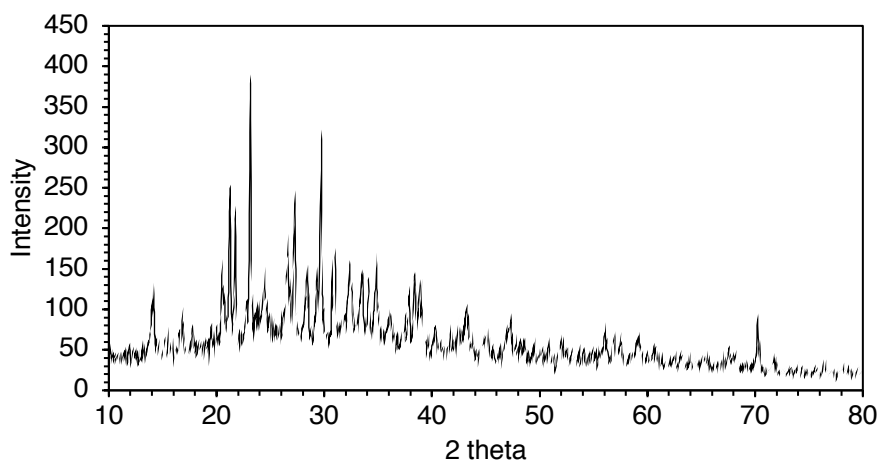


Figure S8. PXRD spectrum of sample A 1.18–9.51 mm size fraction as received.

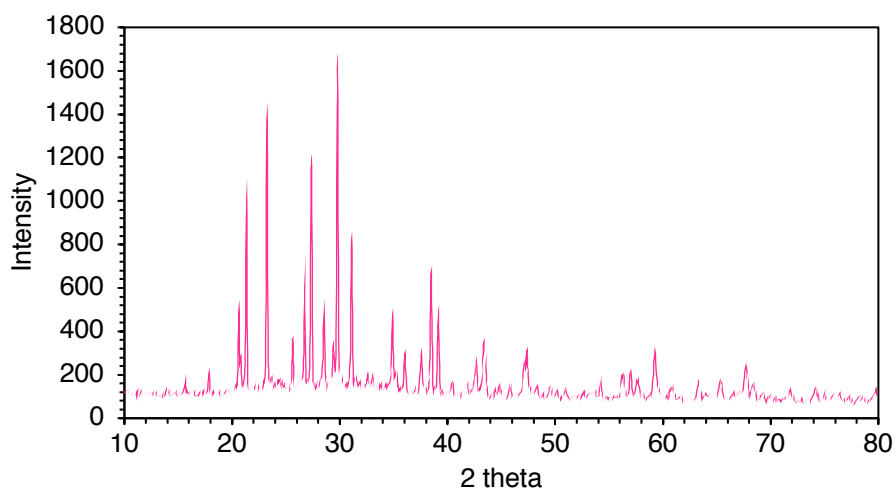


Figure S9. PXRD spectrum of sample A 1.18–9.51 mm size fraction after caustic leaching treatment.

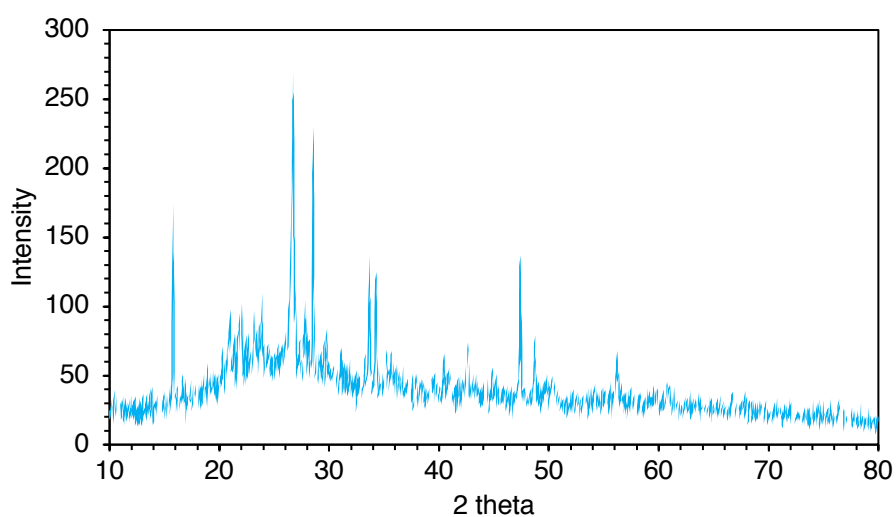


Figure S10. PXRD spectrum of sample A 1.18–9.51 mm size fraction after full leaching treatment.

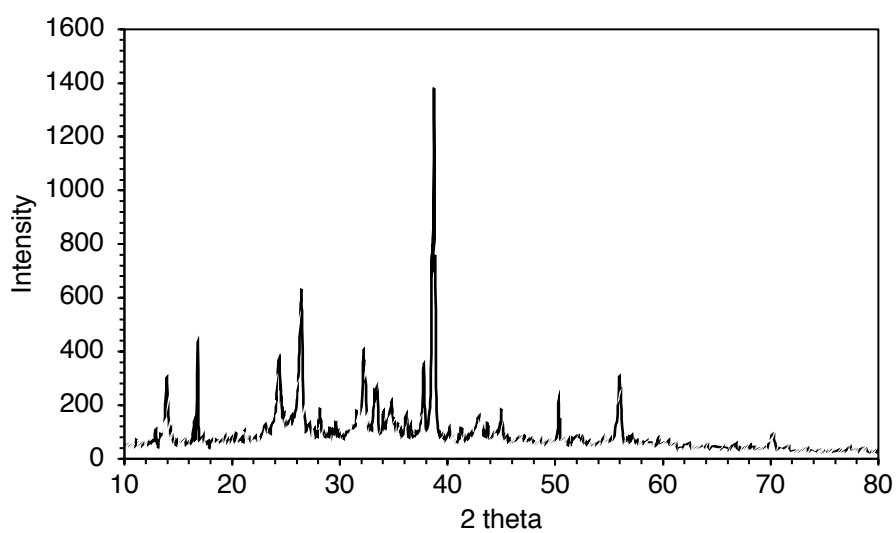


Figure S11. PXRD spectrum of sample B <1.18 mm size fraction as received.

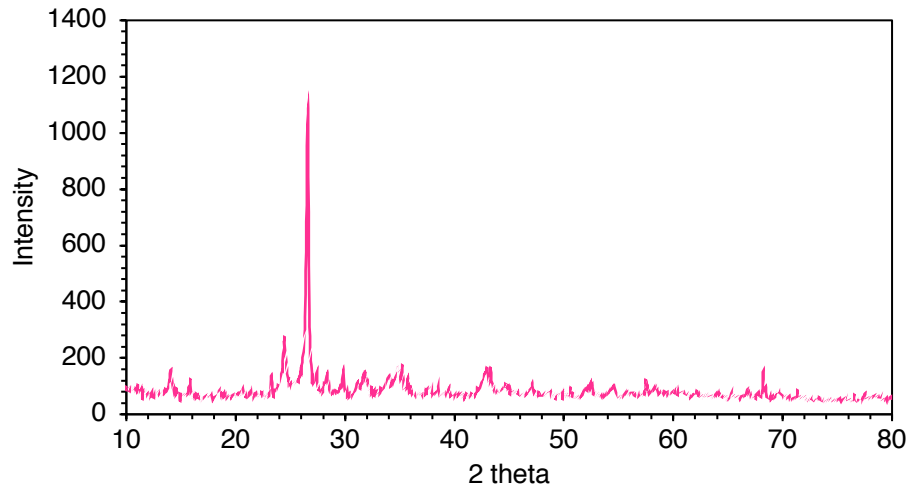


Figure S12. PXRD spectrum of sample B <1.18 mm size fraction after caustic leaching treatment.

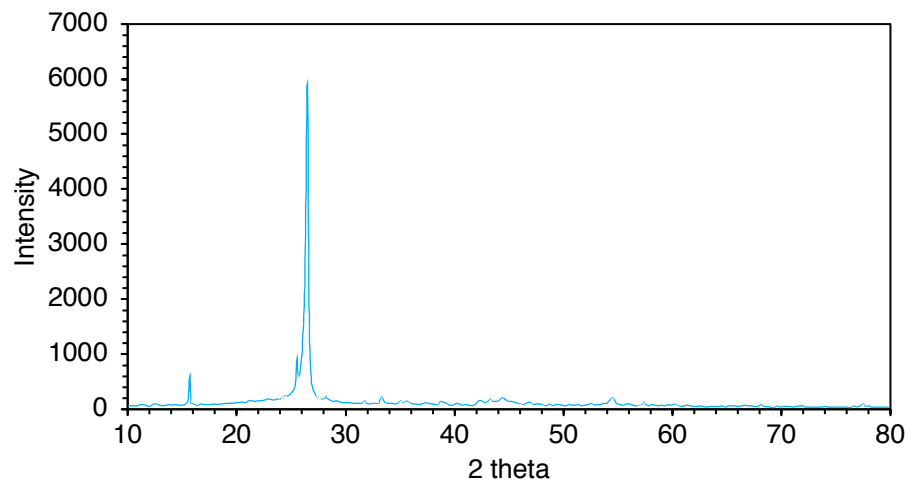


Figure S13. PXRD spectrum of sample B <1.18 mm size fraction after full leaching treatment.

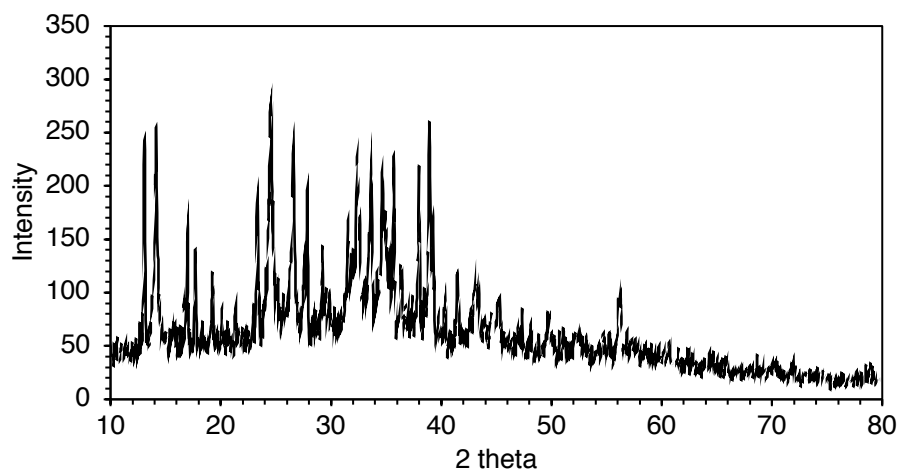


Figure S14. PXRD spectrum of sample B 1.18-9.51 mm size fraction as received.

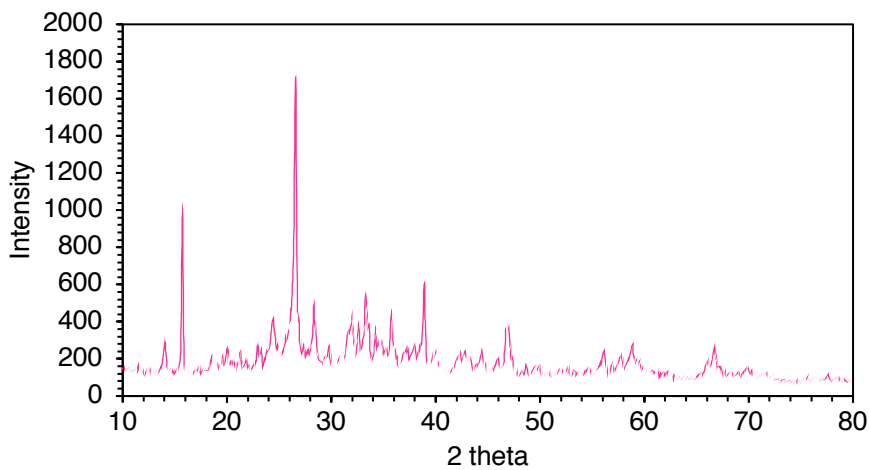


Figure S15. PXRD spectrum of sample B 1.1–9.51 mm size fraction after caustic leaching treatment.

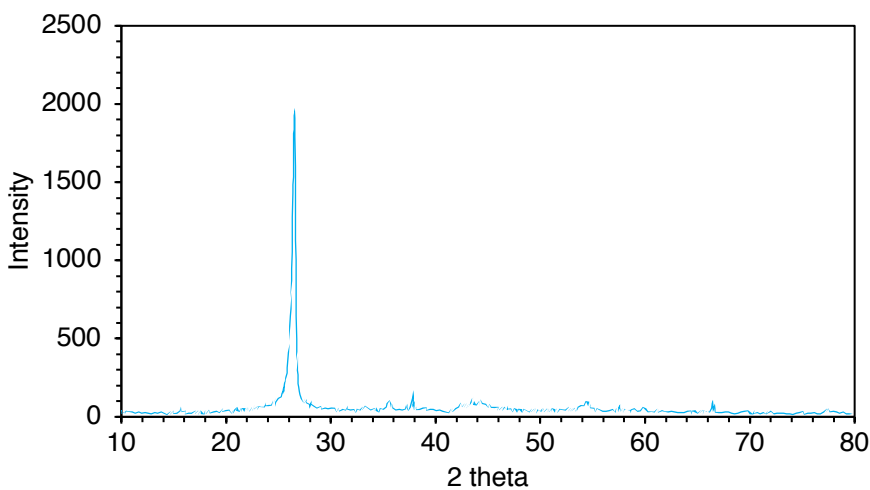


Figure S16. PXRD spectrum of sample B 1.18–9.51 mm size fraction after full leaching treatment.

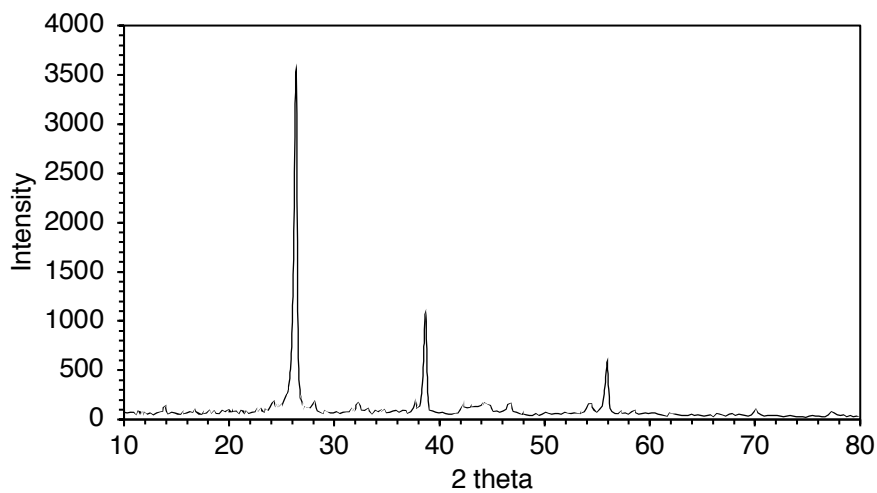


Figure S17. PXRD spectrum of sample C <1.18 mm size fraction as received.

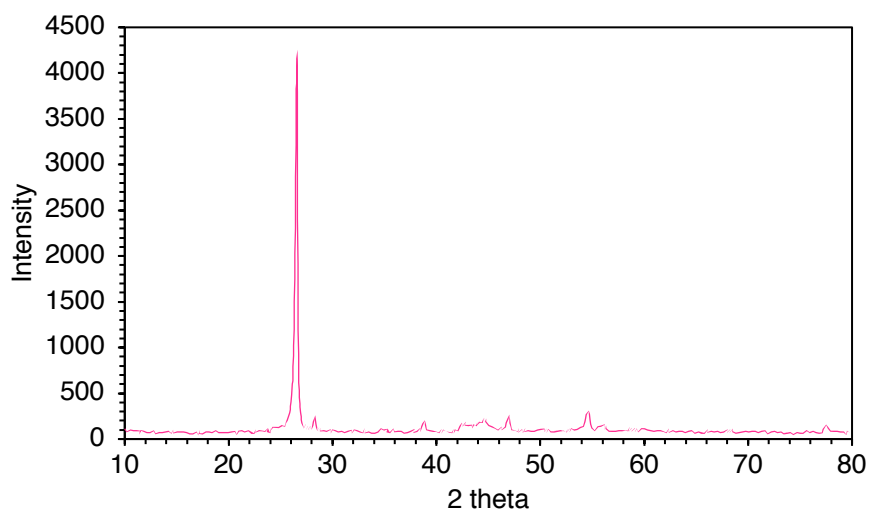


Figure S18. PXRD spectrum of sample C <1.18 mm size fraction after caustic leaching treatment.

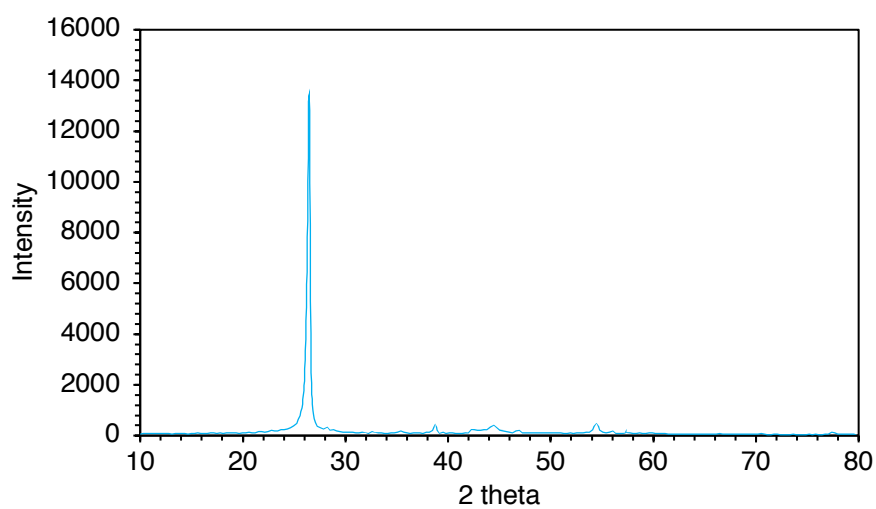


Figure S19. PXRD spectrum of sample C <1.18 mm size fraction after full leaching treatment.

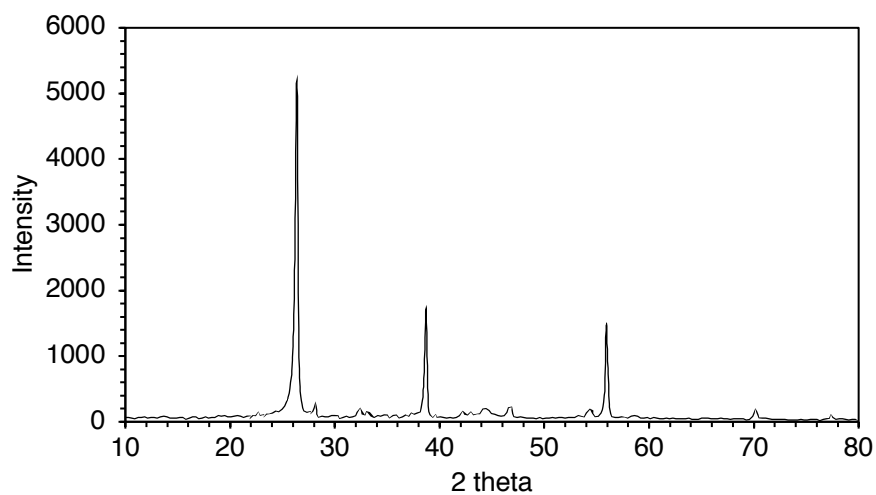


Figure S20. PXRD spectrum of sample C 1.18–9.51 mm size fraction as received.

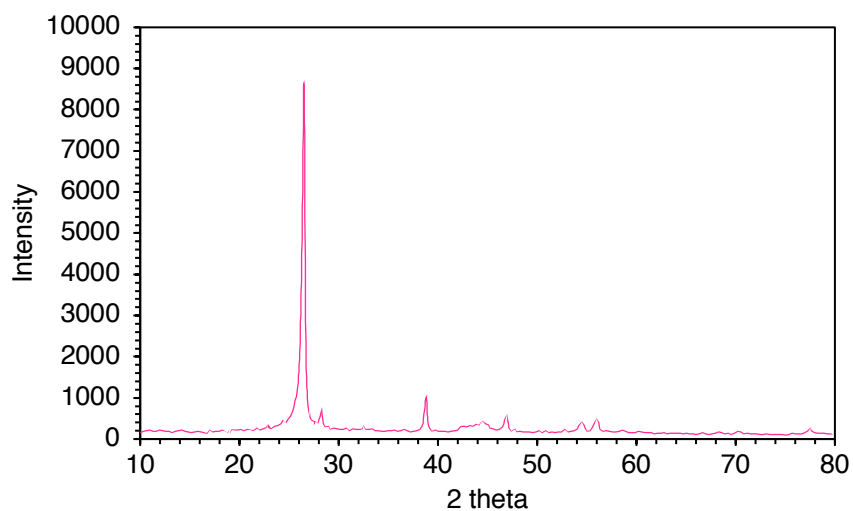


Figure S21. PXRD spectrum of sample C 1.18–9.51 mm size fraction after caustic leaching treatment.

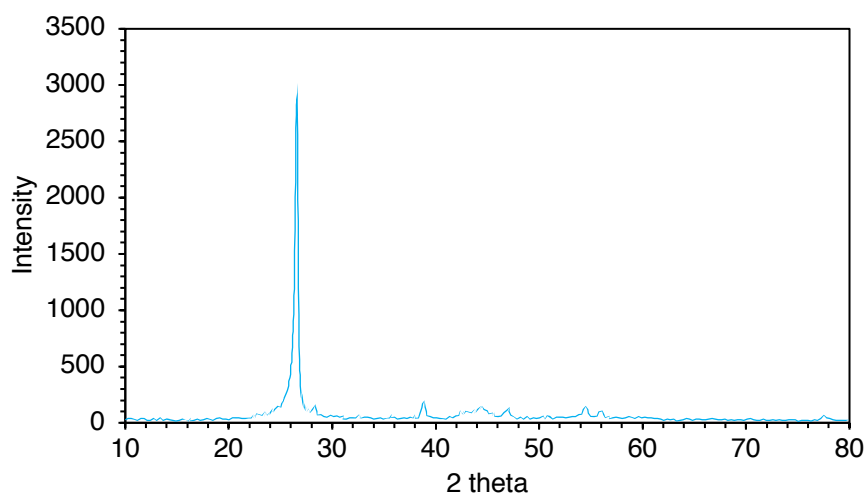


Figure S22. PXRD spectrum of sample C 1.18–9.51 mm size fraction after full leaching treatment.

Scanning electron microscopy (SEM) images

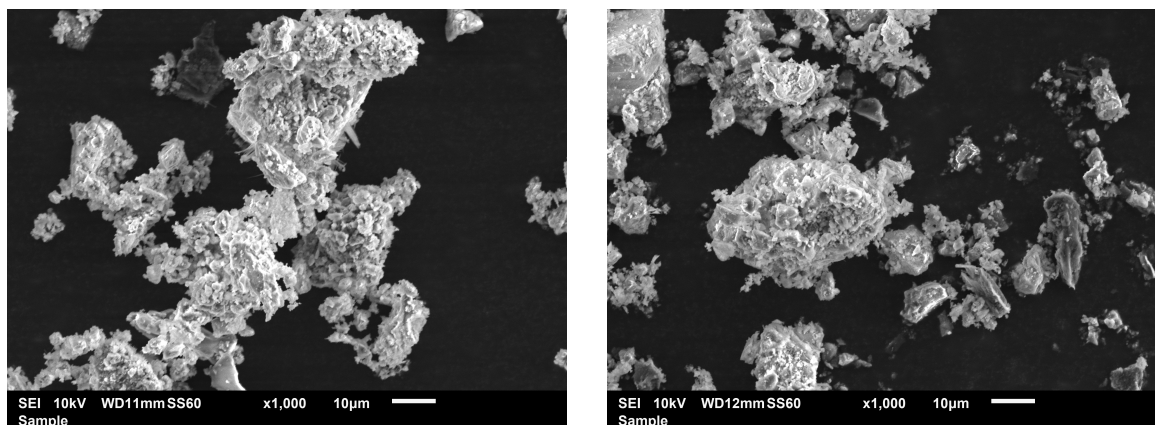


Figure S23. SEM images of sample A <1.18 mm size fraction before (left) and after (right) full leaching treatment.

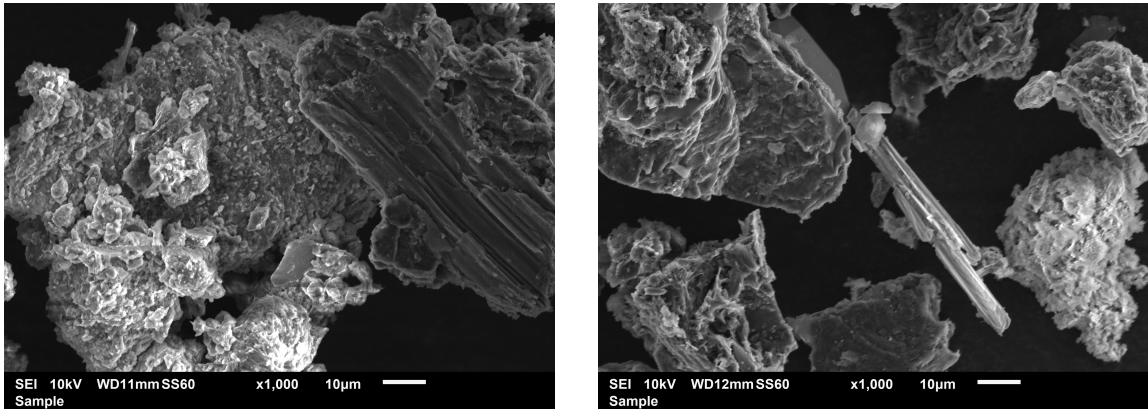


Figure S24. SEM images of sample B <1.18 mm size fraction before (left) and after (right) full leaching treatment.

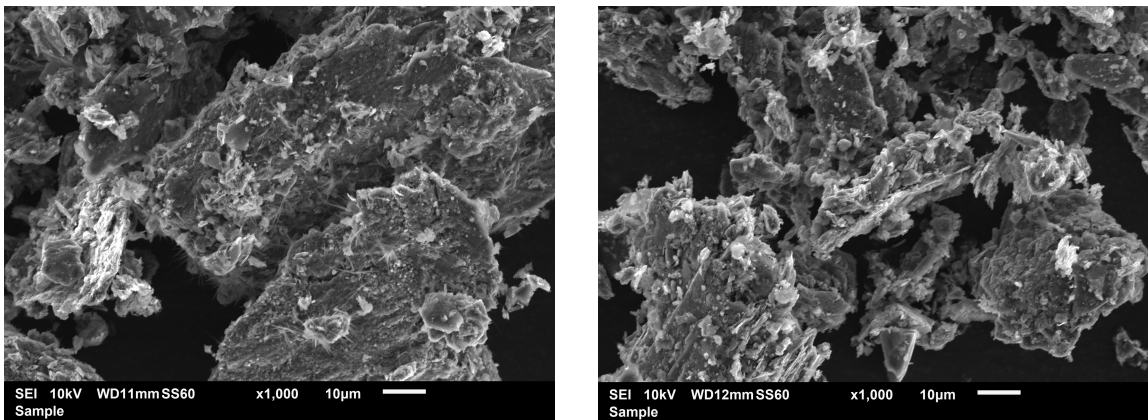


Figure S25. SEM images of sample C <1.18 mm size fraction before (left) and after (right) full leaching treatment.

Energy-dispersive X-ray (EDX) spectra from point analysis (performed in conjunction with SEM imaging)

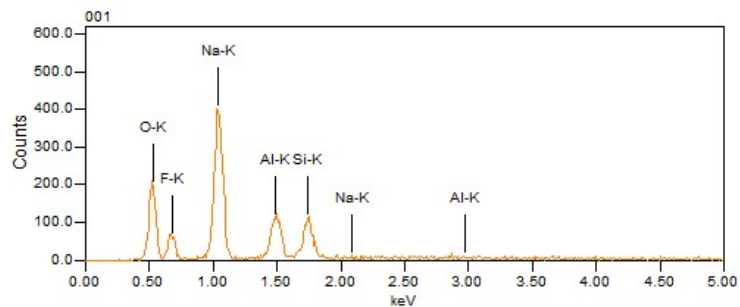


Figure S26. EDX spectrum for point α (cementitious particle) in sample A <1.18 mm size fraction.

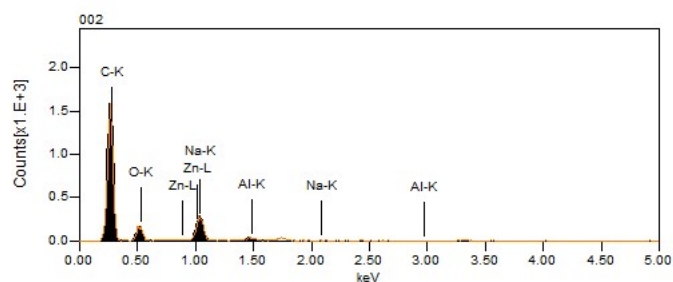


Figure S27. EDX spectrum for point β (graphite particle) in sample A <1.18 mm size fraction.

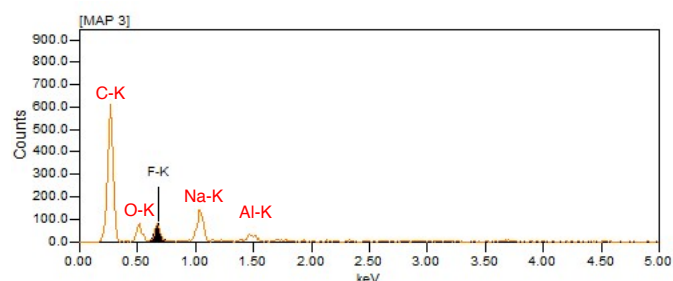


Figure S28. EDX spectrum for point γ (crystalline region) in sample C <1.18 mm size fraction. Peaks labelled in red were manually assigned.

Additional ICP-MS analysis of SPL leachate

Table S1. Quantities of minor chemical species leached from each SPL sample, determined by ICP-MS.

Leaching treatment	Sample										
		Ni	Ba	Be	Cr	Sr	Li	V	Mn	Y	Zn
caustic	A <1.18 mm	< 5	0.480	0.960	21.6	1.44	18.2	16.3	0.480	< 5	77.8
caustic	A 1.18-9.51 mm	< 5	2.46	< 0.5	6.57	0.821	45.6	7.39	1.64	< 5	60.4
caustic	B <1.18 mm	< 5	0.468	1.87	8.89	1.40	34.6	12.6	0.468	< 5	67.4
caustic	B 1.18-9.51 mm	< 5	0.414	3.31	3.31	0.827	26.5	12.8	0.414	< 5	50.9
caustic	C <1.18 mm	< 5	3.92	4.90	20.1	3.43	27.9	7.84	0.490	< 5	67.6
caustic	C 1.18-9.51 mm	< 5	1.30	2.61	6.08	2.61	24.8	3.91	0.434	< 5	44.7
	average	< 5	1.51	2.36	11.1	1.76	29.6	10.2	0.655	< 5	61.5
	Standard deviation		1.42	1.61	7.78	1.05	9.44	4.54	0.485		12.1
acidic	A <1.18 mm	46.3	9.84	3.60	90.0	57.8	34.8	5.28	133.7	6.24	85.2
acidic	A 1.18-9.51 mm	9.45	7.46	3.23	14.9	64.7	32.1	8.71	42.5	7.71	162
acidic	B <1.18 mm	17.2	5.23	5.65	24.1	62.4	32.0	2.51	58.0	4.61	48.4
acidic	B 1.18-9.51 mm	8.02	4.86	2.67	15.8	33.0	16.5	0.729	18.7	2.43	52.7
acidic	C <1.18 mm	28.1	2.14	4.07	37.9	75.9	19.5	3.43	106	2.36	30.2
acidic	C 1.18 mm-9.51 mm	13.6	2.12	6.58	13.4	55.0	21.5	1.91	47.8	1.91	17.4
	average	20.4	5.28	4.30	32.7	58.1	26.1	3.76	67.2	4.21	66.1
	Standard deviation	14.6	3.02	1.51	29.5	14.3	7.79	2.87	43.2	2.38	52.5

Other SPL leaching treatments described in the literature

Table S2. Comparison of SPL leaching treatments previously reported.

SPL cut	Number of stages	Lixiviant(s)	Length of treatment (hr)	Leaching temperature (°C)	Reference
Mixed	2	1 M NaOH (with H ₂ O ₂), 0.5 M H ₂ SO ₄	3 (x 2) + 2	20	This study
First	1	Concentrated chromic acid	< 0.3	100	[7]
Not stated (presumed mixed)	4	Water, HF, H ₂ SiF ₆ , water	Not stated	60 - 90	[8]
Second	1	0.01 M NaOH	18	23	[9]
Not stated (presumed first)	2	2.5 M NaOH, 9.7 M HCl	3 (x 2)	100	[10]
First	2	Water, 0.36 M Al(NO ₃) ₃	4 + 24	25	[11]
First	2	Water, Al anodizing wastewater / 0.7 M H ₂ SO ₄	4 (x 2)	25 - 60	[12]
First	1	NaOH (ultrasound-assisted)	0.67	70	[13]
Not stated (presumed first)	2	Water, Al anodizing wastewater / 1.77 M H ₂ SO ₄	3 (x 2)	80	[14]

Table S3. Composition of SPL from different common smelter cell types [15].

Chemical species (mass %)	Cell type		
	A type prebake	B type prebake	Söderberg
Fluorides	10.9	15.5	18
Cyanides (mg kg ⁻¹)	680	4480	1040
Total aluminium	13.6	11	12.5
Metallic aluminium	1	1	1.9
Carbon	50.2	45.5	38.4
Sodium	12.5	16.3	14.3
Calcium	1.3	2.4	2.4
Iron	2.9	3.1	4.3
Lithium	0.03	0.03	0.6
Titanium	0.23	0.24	0.15
Magnesium	0.23	0.09	0.2

Mixing of caustic and acidic leachates and precipitation

Table S4. Masses of precipitate attained from combination of 25 mL caustic leachate and 25 mL acidic leachate, maintaining pH of ~ 3.

Sample	Precipitate mass (g)
A <1.18 mm	0.1039
A 1.18–9.51 mm	0.0993
B <1.18 mm	0.0661
B 1.18–9.51 mm	0.0929
C <1.18 mm	0.0748
C 1.18–9.51 mm	0.0759

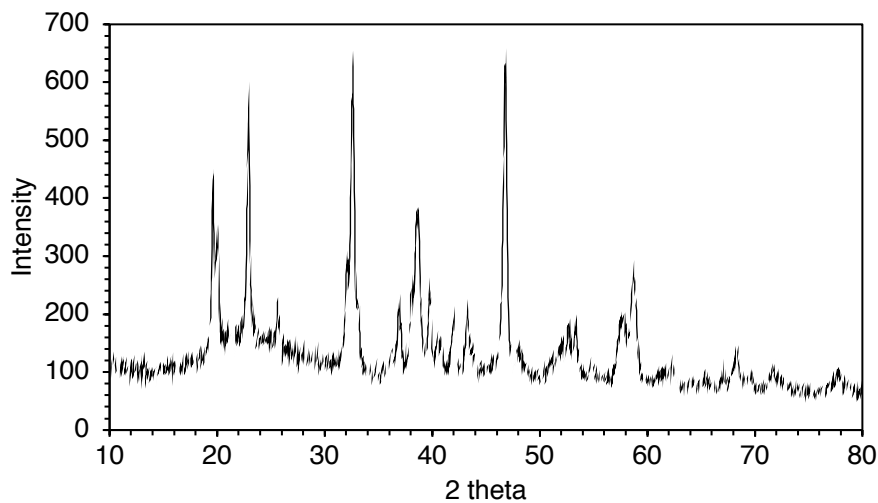


Figure S29. PXRD spectrum of precipitate obtained by mixing caustic and acidic leachates from treatment of sample A, 1.18–9.51 mm fraction.

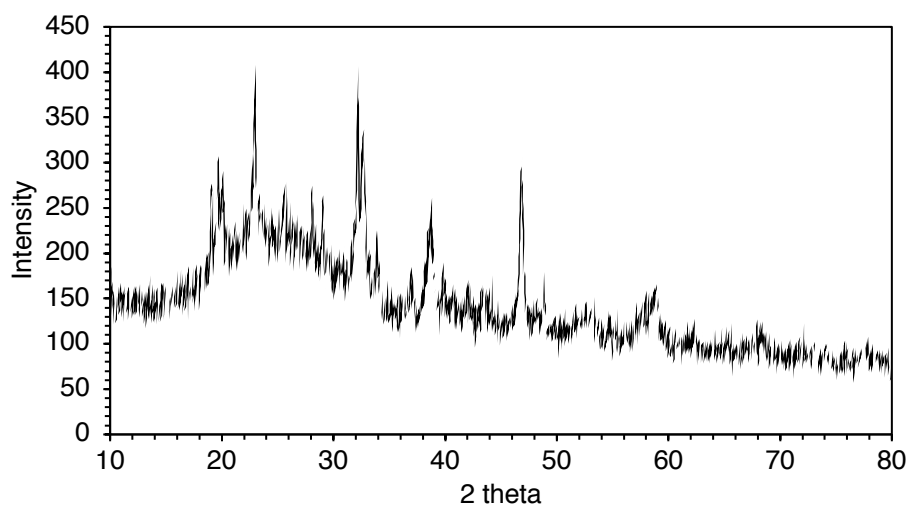


Figure S30. PXRD spectrum of precipitate obtained by mixing caustic and acidic leachates from treatment of sample B, <1.18 mm fraction.

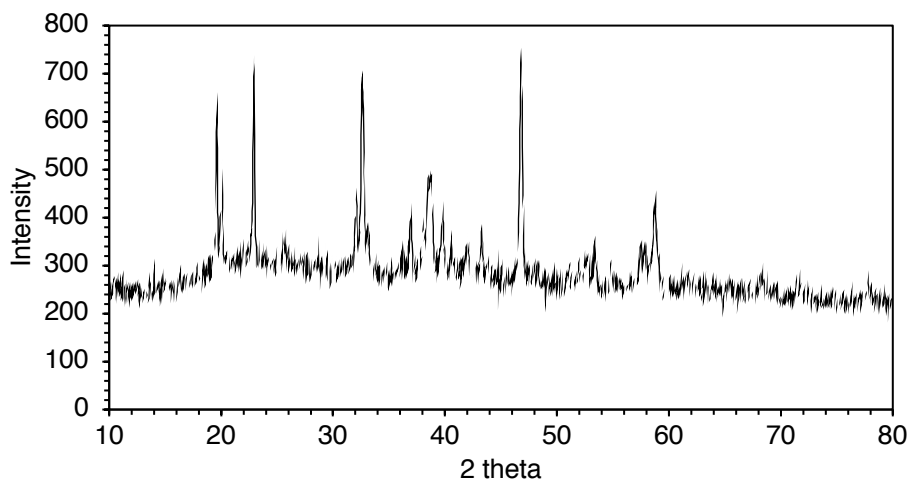


Figure S31. PXRD spectrum of precipitate obtained by mixing caustic and acidic leachates from treatment of sample C, <1.18 mm fraction.

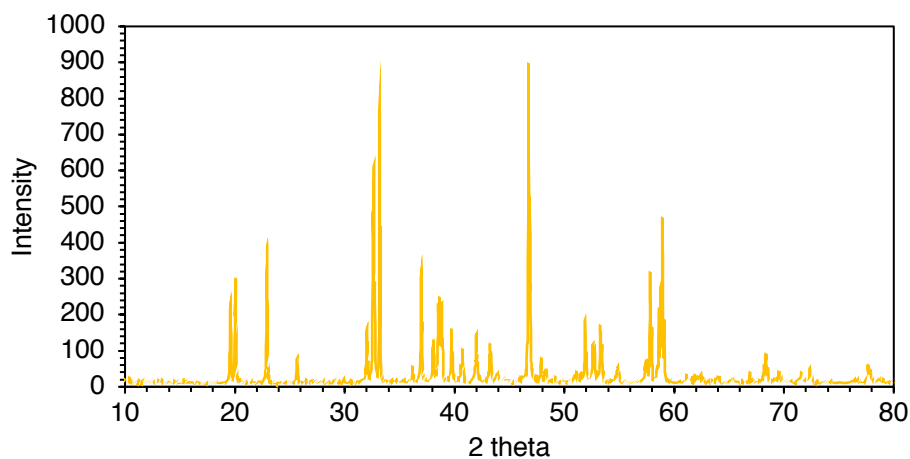


Figure S32. Literature PXRD spectrum of cryolite from the ICDD for comparison [16].

Fixed-bed fluoride column-loading studies and fitting to dynamic models

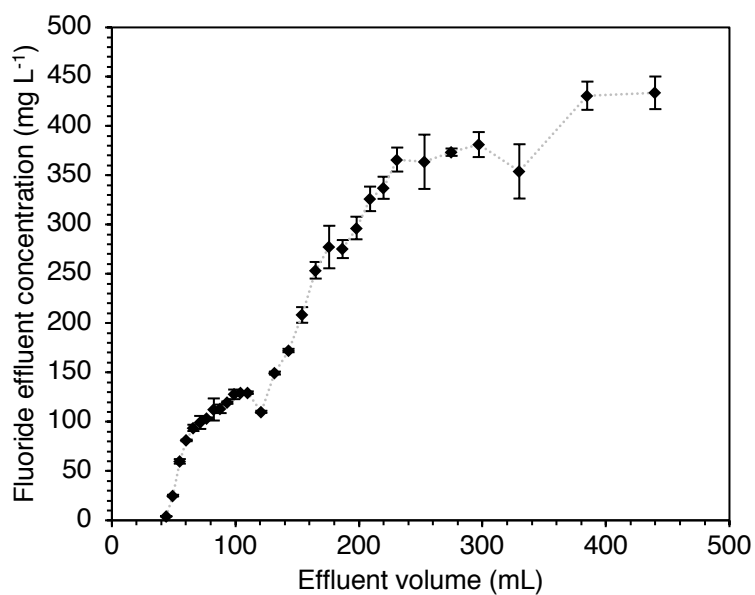


Figure S33. Raw breakthrough data for loading of La-MTS9501 resin column from combined leachate of SPL sample A, 1.18–9.51 mm size fraction. Column volume = 5.50 mL. Resin mass = 1.792 g. Flow rate = 0.50 BV hr⁻¹. T = 20°C.

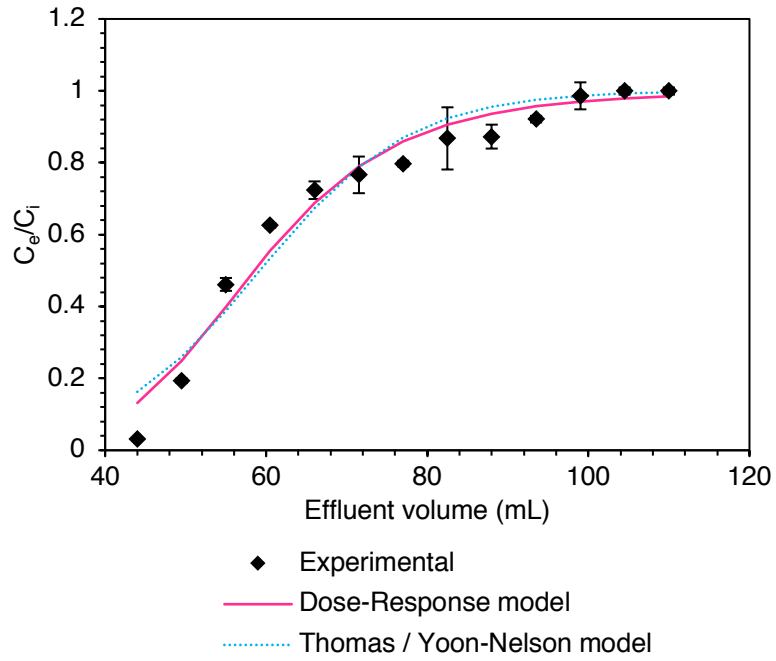


Figure S34. Modelling of first breakthrough region for the above data.

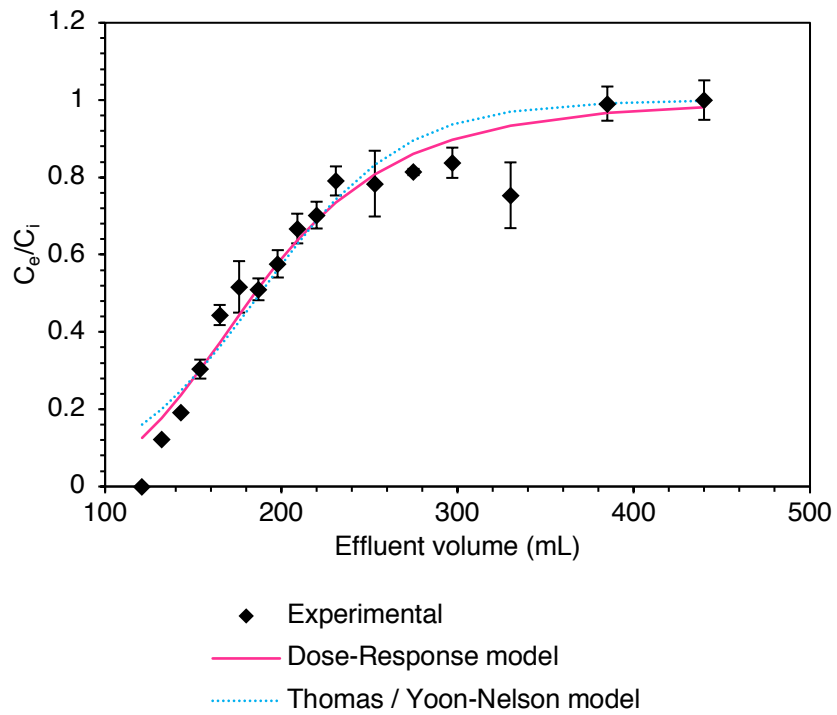


Figure S35. Modelling of second breakthrough region for the above data.

Table S5. Extracted parameters from modelling of breakthrough behaviour for leachates of sample A <1.18 mm and sample A 1.18–9.51 mm. For definition of model parameters, see p3.

Model	Parameter	Breakthrough region	Leachate Sample A < 1.18 mm	Sample A 1.18–9.51 mm
Dose-Response	a	first	5.50 ± 0.60	6.60 ± 0.67
	b	first	74.9 ± 1.7	58.5 ± 1.0
	q ₀	first	5.01 ± 0.11	4.23 ± 0.07
	R ²	first	0.983	0.969
	a	second	5.45 ± 0.47	4.57 ± 0.48
	b	second	262 ± 4	185 ± 4
	q ₀	second	26.7 ± 0.4	33.4 ± 0.7
	R ²	second	0.960	0.947
	R ²	both ^a	0.932	0.959
	Thomas	K _{Th}	first	5.78 ± 0.86 (x 10 ⁻⁵)
q ₀		first	5.10 ± 0.15	4.28 ± 0.09
R ²		first	0.971	0.950
K _{Th}		second	1.02 ± 0.12 (x 10 ⁻⁵)	7.00 ± 0.98 (x 10 ⁻⁶)
q ₀		second	27.1 ± 0.5	34.0 ± 0.9
R ²		second	0.937	0.921
R ²		both ^a	0.942	0.971
Yoon-Nelson	K _{YN}	first	7.56 ± 1.1 (x 10 ⁻²)	0.107 ± 0.015
	T ₅₀	first	76.2 ± 2.2	59.2 ± 1.3
	R ²	first	0.971	0.950
	K _{YN}	second	2.03 ± 0.23 (x 10 ⁻²)	2.47 ± 0.35 (x 10 ⁻²)
	T ₅₀	second	266 ± 5	188 ± 5
	R ²	second	0.937	0.921
	R ²	both ^a	0.942	0.971

^a The R² values for both breakthrough regions are derived from an attempt to fit a single breakthrough curve to the whole dataset.

References

- [1] Robshaw, T.J., Tukra S., Hammond, D.B., Leggett, G.J., Ogden, M.D.: Highly efficient fluoride extraction from simulant leachate of spent potlining via La-loaded chelating resin. An equilibrium study. *J. Hazard. Mater.* 361, 200-209 (2019)
- [2] Robshaw, T.J., Dawson, R., Bonser, K., Ogden, M.D.: Towards the implementation of an ion-exchange system for recovery of fluoride commodity chemicals. Kinetic and dynamic studies. *Chem. Eng. J.* 367, 149-159 (2019)
- [3] Yan, G.Y., Viraraghavan, T., Chen, M.: A new model for heavy metal removal in a biosorption column. *Adsorpt. Sci. Technol.* 19, 25-43 (2001)
- [4] Thomas, H.C.: Heterogeneous ion exchange in a flowing system. *J. Am. Chem. Soc.* 66, 1664-1666 (1944)
- [5] Yoon, Y.H., Nelson, J.H.: Application of gas adsorption kinetics I. A theoretical model for respirator cartridge service life, *Am. Ind. Hyg. Assoc. J.* 45, 509-516 (1984)
- [6] Billo, E.J.: *Excel for Chemists: A Comprehensive Guide*. Wiley, Hoboken, New Jersey (2004)
- [7] Mazumder, B.: Chemical oxidation of spent cathode carbon blocks of aluminium smelter plants for removal of contaminants and recovery of graphite value. *J. Sci. Ind. Res.* 62, 1181-1183 (2003)
- [8] Pong, T.K., Adrien, R.J., Besida, J., O'Donnell, T.A., Wood, D.G.: Spent potlining - A hazardous waste made safe, *Process Saf. Environ. Prot.* 78, 204-208 (2000)
- [9] Silveira, B.I., Dantas, A.E., Blasquez, J.E., Santos, R.K.P.: Characterization of inorganic fraction of spent potliners: evaluation of the cyanides and fluorides content. *J. Hazard. Mater.* 89, 177-183 (2002)

- [10] Shi, Z.-N., Li, W., Hu, X.-W., Ren, B.-J., Gao, B.-L., Wang, Z.-W.: Recovery of carbon and cryolite from spent pot lining of aluminium reduction cells by chemical leaching. *Trans. Nonferrous Met. Soc. China*, 22, 222-227 (2012)
- [11] Lisbona, D.F., Steel, K.M.: Recovery of fluoride values from spent pot-lining: Precipitation of an aluminium hydroxyfluoride hydrate product. *Sep. Purif. Technol.* 61, 182-192 (2008)
- [12] Lisbona, D.F., Somerfield, C., Steel, K.M.: Leaching of spent pot-lining with aluminum anodizing wastewaters: Fluoride extraction and thermodynamic modeling of aqueous speciation. *Ind. Eng. Chem. Res.* 51, 8366-8377 (2012)
- [13] Xiao, J., Yuan, J., Tian, Z.L., Yang, K., Yao, Z., Yu, B.L., Zhang, L.Y.: Comparison of ultrasound-assisted and traditional caustic leaching of spent cathode carbon (SCC) from aluminum electrolysis. *Ultrason. Sonochemistry* 40, 21-29 (2018)
- [14] Li, X.M., Yin, W.D., Fang, Z., Liu, Q.H., Cui, Y.R., Zhao, J.X., Jia, H.: Recovery of Carbon and Valuable Components from Spent Pot Lining by Leaching with Acidic Aluminum Anodizing Wastewaters. *Metallurgical Mater. Trans. B - Process Metall. Mater. Process. Sci.* 50, 914-923 (2019)
- [15] Holywell, G., Bréault, R.: An Overview of Useful Methods to Treat, Recover, or Recycle Spent Potlining. *J. Miner. Met. Mater. Soc.* 65, 1441-1451 (2013)
- [16] Fawcett, T.G., Needham, F., Crowder, C., Kabekkodu, S.: Advanced materials analysis using the powder diffraction file. 10th National Conference on X-ray Diffraction and ICDD Workshop. Shanghai, China (2009)